

DRAFT: NCT

RA

2022-02-15

1 Introduction

TODO(1): intro

We are particularly interested in the nuclear-to-cytoplasmic contrast (henceforth, N:C contrast) of certain molecular species at steady state: $\text{Ran} \cdot \text{GTP}$, $\text{Imp}\beta$, CAS, and NLS.

Abbreviations. FG-nups = FG-nucleoporins; NCT = nucleocytoplasmic transport; NPC = nuclear pore complex; NE = nuclear envelope; IBB = importin beta binding; ODE = ordinary differential equations; SPR = surface plasmon resonance;

2 NCT models

2.1 GSR'03 model of NCT

Ran gradient. The Ran gradient, i.e. the nuclear accumulation of $\text{Ran} \cdot \text{GTP}$, is the base layer of nucleocytoplasmic transport. We implement it as the “minimal Ran gradient system” from [GSR03]. The equations are recapitulated in §3.1 and the constants are collected in Table 2. Following [GSR03], the “dynamic capacity” Ex is an optional maximal steady-state (positive) flux of nuclear $\text{Ran} \cdot \text{GTP}$ to cytoplasmic $\text{Ran} \cdot \text{GDP}$, which we determine using the additional equation (19). The fluxes are in units of concentration/time ($\mu\text{M}/\text{s}$). The ones across the nuclear boundary have positive sign when exiting the nucleus and are normalized to the nuclear volume. Thus, the *amount* exiting the nucleus per unit of time is $\text{flux} \times V_{\text{nuc}}$.

Simulating the ODE across the scenarios of [GSR03] we obtain results that are sufficiently close to the original, see Table 3. Importantly, an order of 1000-fold nuclear enrichment of $\text{Ran} \cdot \text{GTP}$ is sustained in steady-state. Moreover, the dynamic capacity clocks in at around $0.6 \mu\text{M}/\text{s}$ in most cases, meaning the Ran gradient is established within seconds. Therefore, we will replace the whole Ran gradient layer by a virtual pump



This rate is chosen conservatively (a concentration of 1 μM of cytoplasmic $\text{Ran} \cdot \text{GDP}$ generates a flux of 0.1 $\mu\text{M/s}$) but will be sufficient for our purposes.

Code [#1](#).

Coupling to Imp β -mediated transport. A coupling of the Ran gradient to importin-cargo transport was proposed in [GSR03, Fig. 6A]. We now formulate a version of it. The following equations comprise the handling of cargo by Imp β in the cytoplasm,

$$\frac{d}{dt}[\text{Imp}\beta \cdot \text{Ran} \cdot \text{GTP}]_{\text{cyt}} = -R_{\text{cyt}} + F_{\text{Imp}\beta \cdot \text{Ran} \cdot \text{GTP}} \frac{V_{\text{nuc}}}{V_{\text{cyt}}} - \text{GAP}_{\text{Imp}\beta} + \text{Knockoff}_{\text{cyt}} \quad (2a)$$

$$\frac{d}{dt}[\text{Imp}\beta]_{\text{cyt}} = +R_{\text{cyt}} + C_{\text{cyt}} + F_{\text{Imp}\beta} \frac{V_{\text{nuc}}}{V_{\text{cyt}}} + \text{GAP}_{\text{Imp}\beta} \quad (2b)$$

$$\frac{d}{dt}[\text{Imp}\beta \cdot \text{Cargo}]_{\text{cyt}} = -C_{\text{cyt}} + F_{\text{Imp}\beta \cdot \text{Cargo}} \frac{V_{\text{nuc}}}{V_{\text{cyt}}} - \text{Knockoff}_{\text{cyt}} \quad (2c)$$

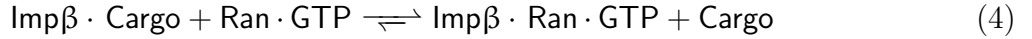
$$\frac{d}{dt}[\text{Cargo}]_{\text{cyt}} = +C_{\text{cyt}} + F_{\text{Cargo}} \frac{V_{\text{nuc}}}{V_{\text{cyt}}} + \text{Knockoff}_{\text{cyt}} \quad (2d)$$

with the fluxes

$$R_{\text{cyt}} := -k_{\text{on}}^{\text{R}}[\text{Imp}\beta][\text{Ran} \cdot \text{GTP}]_{\text{cyt}} + k_{\text{off}}^{\text{R}}[\text{Imp}\beta \cdot \text{Ran} \cdot \text{GTP}]_{\text{cyt}} \quad (3a)$$

$$C_{\text{cyt}} := -k_{\text{on}}^{\text{C}}[\text{Imp}\beta][\text{Cargo}]_{\text{cyt}} + k_{\text{off}}^{\text{C}}[\text{Imp}\beta \cdot \text{Cargo}]_{\text{cyt}}. \quad (3b)$$

The forward flux of the reaction



is called **Knockoff**. It is modeled as a one-way reaction with forward rate k_{knockoff} . The GSR equations are modified accordingly:

$$\frac{d}{dt}[\text{Ran} \cdot \text{GDP}]_{\text{cyt}} = (13a) + \text{GAP}_{\text{Imp}\beta} \quad (13a')$$

$$\frac{d}{dt}[\text{Ran} \cdot \text{GTP}]_{\text{cyt}} = (13b) + R_{\text{cyt}} - \text{Knockoff}_{\text{cyt}} \quad (13b')$$

Analogous nuclear equations (without GAP) are implemented but are omitted here. Analogously to (17a)/(17b) we have the additional nuclear-to-cytoplasmic diffusion fluxes

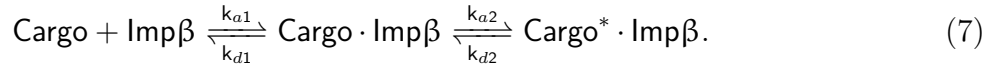
$$F_{\text{Imp}\beta \cdot \text{Ran} \cdot \text{GTP}}, \quad F_{\text{Imp}\beta}, \quad F_{\text{Imp}\beta \cdot \text{Cargo}}, \quad F_{\text{Cargo}} \quad (5)$$

with the permeability constants given in Table 1.

SPR experiments of [Cat+01] indicated that the IBB domain of importin- α binds importin- β and undergoes a conformational change,



We therefore assume the analogous reaction



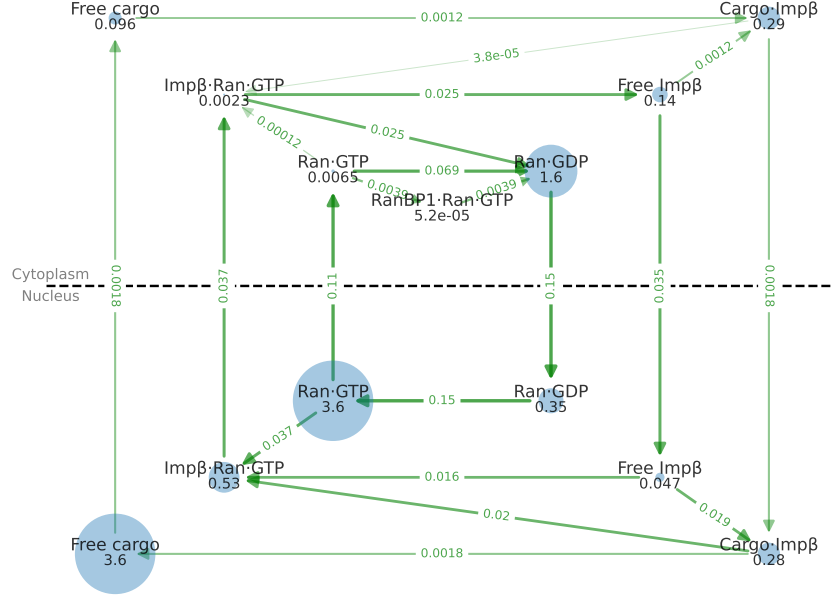


Figure 1: Steady-state of the transport system from §2.1 with conditions of Table 1. The free cargo shows 37-fold accumulation in the nucleus; total nuclear to total cytoplasmic cargo is 10-fold. Units are μM for species and $\mu\text{M s}^{-1}$ for fluxes. Initial conditions: $[\text{Ran} \cdot \text{GDP}]_{\text{cyt}} = 5 \mu\text{M}$, $[\text{Imp}\beta]_{\text{cyt}} = 1 \mu\text{M}$, $[\text{Cargo}]_{\text{cyt}} = 3 \mu\text{M}$, all else zero.

Examples of the kinetic constants are available in [Cat+01, Table I], e.g.,

$$k_{a1} = 0.11 \mu\text{M}^{-1} \text{s}^{-1}, \quad k_{d1} = 0.024 \text{s}^{-1}, \quad k_{a2} = 0.024 \text{s}^{-1}, \quad k_{d2} = 7.4 \times 10^{-4} \text{s}^{-1}, \quad (8)$$

for an IBB domain binding to Imp β . The intermediate state in (6) is transient on a moderately relevant time-scale (code #2). Therefore, in the present model we lump the complexed states together and take $k_{\text{on}}^{\text{C}} := k_{a1}$ and $k_{\text{off}}^{\text{C}} := k_{d1} \frac{k_{d2}}{k_{a2} + k_{d2}}$ as the effective kinetic constants for (3b), cf. Table 1.

With the constants from Table 1, the steady-state of the model (reached after some 10^4s) is reported in Fig. 1. Nuclear accumulation of free cargo is 37-fold. Sensitivity analysis shows that, in relative terms, the final nuclear concentration of free cargo depends most strongly on k_{knockoff} . Doubling k_{knockoff} almost doubles the nuclear concentration. Code #3.

This model predicts a slight accumulation of Imp β in the nucleus, with Imp β ·Ran·GTP contributing most of the excess. We improve on it in §2.3.

2.2 GTP hydrolysis and role of RanBP1

According to [LM97, Fig. 4A], Imp β blocks hydrolysis of Ran·GTP by RanGAP but RanBP1 rescues it for most part. Similarly, [BG97] showed that RanBP1 transiently detaches Ran from the complex Kap·Ran·GTP (where Kap is some karyopherin), whereupon hydrolysis

(3a)	$k_{\text{on}}^{\text{R}} = 0.096 \mu\text{M}^{-1} \text{s}^{-1}$, $k_{\text{off}}^{\text{R}} = 4.8 \times 10^{-6} \text{s}^{-1}$	[GSR03, Supp. Table A], [RM05, Table II]
(3b)	$k_{\text{on}}^{\text{C}} = 0.11 \mu\text{M}^{-1} \text{s}^{-1}$, $k_{\text{off}}^{\text{C}} = 7.2 \times 10^{-4} \text{s}^{-1}$	[Cat+01, Table I], [RM05, Table II]
(4)	$k_{\text{knockoff}} = 2 \times 10^{-2} \mu\text{M}^{-1} \text{s}^{-1}$	[RM05, Table II]
(5)	$D_{\text{Imp}\beta \cdot \text{Ran} \cdot \text{GTP}} = 0.07 \text{s}^{-1}$, $D_{\text{Imp}\beta} = 0.4 \text{s}^{-1}$ $D_{\text{Imp}\beta \cdot \text{Cargo}} = 0.25 \text{s}^{-1}$, $D_{\text{Cargo}} = 5 \times 10^{-4} \text{s}^{-1}$	[RM05, Table III]

Table 1: Constants for the $\text{Imp}\beta$ -mediated transport from §2.1.

by RanGAP disassembles the complex; and that efficient disassembly of $\text{Imp}\beta \cdot \text{Ran} \cdot \text{GTP}$ required RanBP1 and $\text{Imp}\alpha$ [BG97, §3.2, cf. Fig. 4], [FBR97]. Importantly, Kaps and RanBP1 bind Ran at distinct sites [BG97, p.253].

Further, [See+03, Fig. 13] characterizes the kinetics of the formation of the complex between $\text{Ran} \cdot \text{GTP}$, RanBP1 and RanGAP and the hydrolysis. In particular, the release rate of the γ -phosphate, on the order of 10s^{-1} in [See+03, Fig. 13], is barely influenced by RanBP1 , which instead stimulates the association of Ran with RanGAP . A computational model of hydrolysis with these parameters qualitatively reproduces the experimental data from [LM97, Fig. 4A]. We omit the details that can be found in Code #4.

For simplicity, we will take the constant

$$\text{GTP hydrolysis rate of } 0.1 \text{s}^{-1} \quad (9)$$

for all cytoplasmic-side species containing $\text{Ran} \cdot \text{GTP}$, and no GTP hydrolysis elsewhere. This should be compared with the effective Ran gradient rate (1).

TODO(2): cf [KKL21] citing [Kle+95a] or [Kle+95b]

2.3 NPC as compartment

Introduction. It has been observed [KKL21] that $\text{Imp}\beta$ accumulates inside the NPCs as they bind to the FG-nups, suggesting a regulatory role, and possibly shuttling the cargo across the pore repeatedly. To account for this we propose a model with cytoplasm, nucleus and the NPCs as three compartments. The following dual observation is essential (cf. [Hof20]):

1. cytoplasmic and nuclear species initially react with NPC components in proportion to the number of NPCs, and
2. the observed fluorescence signal from Kaps accumulating inside the NPCs scales with the total volume or the capacity of the NPC channel (rather than their number).

The model includes the following main components:

- $\text{Imp}\beta$ ($\text{Kap}\beta 1$) and the cargo adapter $\text{Imp}\alpha$ ($\text{Kap}\alpha$). For simplicity, we do not model individual variants or isoforms, cf. [KKL21, p. 2].

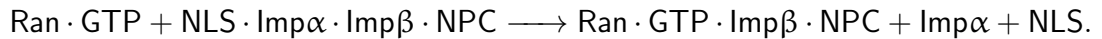
- Generic NLS cargo, by itself unable to transition the nuclear envelope efficiently. Requires the $\text{Imp}\alpha$ to be captured by $\text{Imp}\beta$.
- CAS (Exp2, Xpo2) **TODO(3): on CAS**
- The NPCs are described as vacant NPC channel space, the cytoplasm-facing opening NPC(c) and the nucleus-facing opening NPC(n). To transition the nuclear pore, a species has to bind to the opening, transition into the channel, bind to the other opening, and unbind on the other side. This allows us to model the capacity of the NPC and the dwelling time (but we make no distinction between different transiting species). There is no directionality, i.e. a species currently residing in the channel is equally likely to bind to either opening next.
- $\text{Ran} \cdot \text{GTP}$ in the nucleus and $\text{Ran} \cdot \text{GDP}$ in the cytoplasm. The consumption of $\text{Ran} \cdot \text{GTP}$ that have transitioned to the cytoplasmic side by hydrolysis is compensated by an effective pump as in (1). The hydrolysis itself is described by one effective kinetic rate as in (9).

An overview of the model is shown in Fig. 2. The code is found in Code #5. The computational results for this model are summarized in Fig. 3. For details visit the URL

<https://numpde.github.io/nct1/code/20211018-Appli/checkpoint/20220209-143110/> (10)

Main reactions. Here we comment on the main reactions of the model. For the complete set we refer to Fig. 2 as well as the URL (10).

- The nuclear $\text{Ran} \cdot \text{GTP}$ is converted directly to cytoplasmic $\text{Ran} \cdot \text{GDP}$ as in Eqn. (1).
- The $\text{Imp}\beta$ can shuttle on its own through the NPC or in complex with $\text{Imp}\alpha$. We assume that the complex does not form on the nuclear side (due to nuclear $\text{Ran} \cdot \text{GEF}$, which is not modeled explicitly).
- The cytoplasmic NLS cargo associates with free cytoplasmic $\text{Imp}\alpha \cdot \text{Imp}\beta$ before binding to the cytoplasmic side of the NPC, or with those already attached there. Once the complex is shuttled to the nuclear side, the “knockoff” reaction releases the cargo (the suffix (n) is omitted):



Thereupon, the complex $\text{Ran} \cdot \text{GTP} \cdot \text{Imp}\beta$ can transition from the nuclear to the cytoplasmic side to be hydrolyzed as in Eqn. (9).

- Like $\text{Imp}\beta$, CAS can shuttle through the NPC. On the nuclear side, it can first bind to $\text{Ran} \cdot \text{GTP}$ then form the $\text{Imp}\alpha \cdot \text{CAS} \cdot \text{Ran} \cdot \text{GTP}$ complex. This complex can shuttle through the NPC, and it is disassembled on the cytoplasmic side by the hydrolysis reaction (9).

Baseline parameters. Here we comment on the choice of selected model parameters, such as concentrations and kinetic rates. For the complete set see the URL (10).

We estimate the total NPC channel capacity as 2000 NPCs per nuclear envelope (BioNumbers #111130) times 300 Kaps per NPC **TODO(4): refs for those numbers**. Note that

$$1 \text{ pL} \times 1 \text{ }\mu\text{M} \approx 300 \times 2000 \text{ units}, \quad (11)$$

which implies a concentration of 1 μM in a computational volume of 1 pL. The computation itself is performed in amounts (rather than concentration), so to convert to apparent concentration of Kaps at the NE we estimate **TODO(5): automate insertion of this volume**

$$\text{the volume of apparent NE fluorescence as } 0.01 \text{ pL}. \quad (12)$$

For the initial concentration of **Imp β** we take 5 μM in nucleus and cytoplasm based on [KKL21, Fig. 4] / [NPW19, Fig. 4a].

[YM06]

For the initial concentration of **Imp α** we considered taking 4 μM throughout the cell, slightly below that of **Imp β** , based on the immunoblots of [ZAH13, Fig. 7] and the mass spectrometry measurements for **KPNAs** from [Wüh+14, Table S5]. However, this seemed incompatible with other parameters in that the steady state showed unexpected results, e.g. the NLS remained tied to **Imp α** and nearly equipartitioned between nuclear and cytoplasmic sides. We settled on the **Imp α** concentration of 0.4 μM for the baseline model.

[KKL21] [Kir+15]

TODO(6): complete section

Variants. We have defined a handful of scenarios to illustrate how parameter choice affects the steady-states. The results are summarized in Fig. 3. All parameter changes are with respect to the baseline scenario, and are reported at the URL (10).

1. Decrease **Imp β** tenfold. **TODO(7): Why**
2. Increase the number of NPCs tenfold. **TODO(8): Why**
3. Increase **Imp α** tenfold.
4. Decrease **Imp α** tenfold.
5. Turn off **Ran**·GTP regeneration, starting from the baseline scenario. We obtain a breakdown of N:C contrast for all species, as expected.

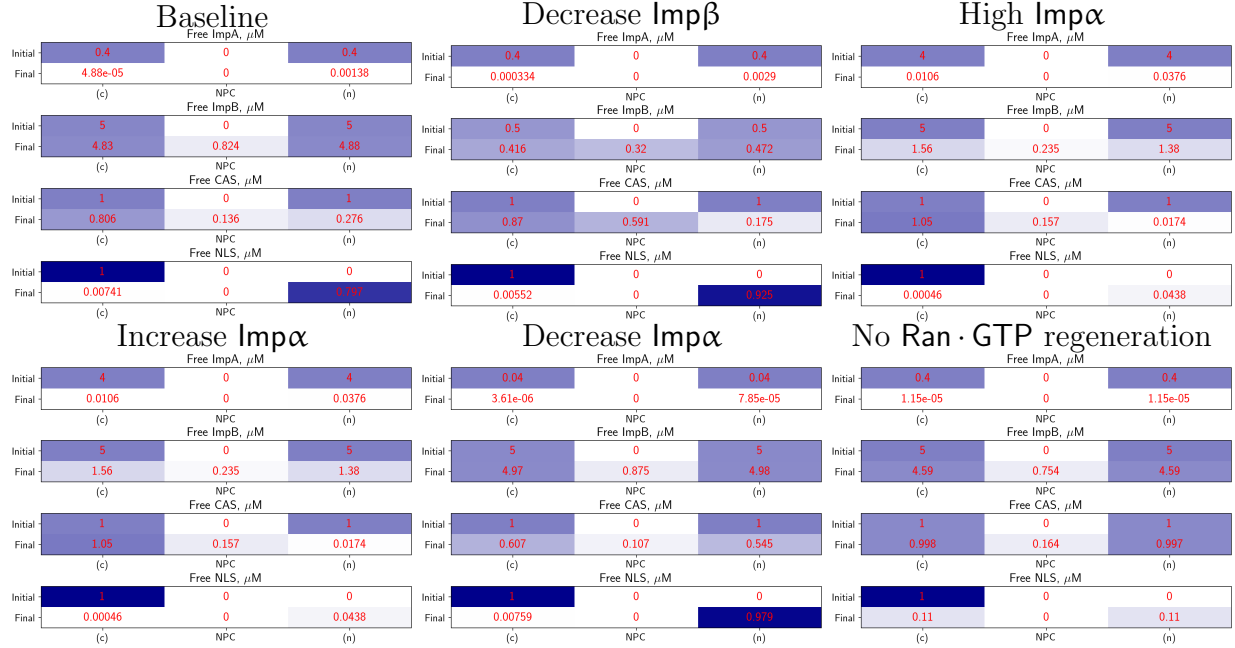


Figure 3: Initial states and steady-states for the model “NPC as compartment” from §2.3. For more full-size figures, see the URL (10).

References

- [Bis+95] F. R. Bischoff, H. Krebber, E. Smirnova, W. Dong, and H. Ponstingl. “Co-activation of RanGTPase and inhibition of GTP dissociation by Ran–GTP binding protein RanBP1”. In: *The EMBO Journal* 14.4 (Feb. 1995), pp. 705–715. DOI: [10.1002/j.1460-2075.1995.tb07049.x](https://doi.org/10.1002/j.1460-2075.1995.tb07049.x) (cit. on p. 11).
- [Kle+95a] C. Klebe, F. R. Bischoff, H. Ponstingl, and A. Wittinghofer. “Interaction of the Nuclear GTP-Binding Protein Ran with Its Regulatory Proteins RCC1 and RanGAP1”. In: *Biochemistry* 34.2 (Jan. 1995), pp. 639–647. DOI: [10.1021/bi00002a031](https://doi.org/10.1021/bi00002a031) (cit. on pp. 4, 13).
- [Kle+95b] C. Klebe, H. Prinz, A. Wittinghofer, and R. S. Goody. “The Kinetic Mechanism of Ran-Nucleotide Exchange Catalyzed by RCC1”. In: *Biochemistry* 34.39 (Oct. 1995), pp. 12543–12552. DOI: [10.1021/bi00039a008](https://doi.org/10.1021/bi00039a008) (cit. on pp. 4, 11–13).
- [BG97] F. Bischoff and D. Görlich. “RanBP1 is crucial for the release of RanGTP from importin β -related nuclear transport factors”. In: *FEBS Letters* 419.2-3 (Dec. 1997), pp. 249–254. DOI: [10.1016/s0014-5793\(97\)01467-1](https://doi.org/10.1016/s0014-5793(97)01467-1) (cit. on pp. 3, 4).
- [FBR97] M. Floer, G. Blobel, and M. Rexach. “Disassembly of RanGTP-Karyopherin β Complex, an Intermediate in Nuclear Protein Import”. In: *Journal of Biological Chemistry* 272.31 (Aug. 1997), pp. 19538–19546. DOI: [10.1074/jbc.272.31.19538](https://doi.org/10.1074/jbc.272.31.19538) (cit. on p. 4).
- [LM97] K. M. Lounsbury and I. G. Macara. “Ran-binding Protein 1 (RanBP1) Forms a Ternary Complex with Ran and Karyopherin β and Reduces Ran GTPase-activating

- Protein (RanGAP) Inhibition by Karyopherin β ". In: *Journal of Biological Chemistry* 272.1 (Jan. 1997), pp. 551–555. DOI: [10.1074/jbc.272.1.551](https://doi.org/10.1074/jbc.272.1.551) (cit. on pp. 3, 4).
- [Cat+01] B. Catimel, T. Teh, M. R. Fontes, I. G. Jennings, D. A. Jans, G. J. Howlett, E. C. Nice, and B. Kobe. "Biophysical Characterization of Interactions Involving Importin- α during Nuclear Import". In: *Journal of Biological Chemistry* 276.36 (Sept. 2001), pp. 34189–34198. DOI: [10.1074/jbc.m103531200](https://doi.org/10.1074/jbc.m103531200) (cit. on pp. 2–4).
- [GSR03] D. Görlich, M. J. Seewald, and K. Ribbeck. "Characterization of Ran-driven cargo transport and the RanGTPase system by kinetic measurements and computer simulation". In: *The EMBO Journal* 22.5 (Mar. 2003), pp. 1088–1100. DOI: [10.1093/emboj/cdg113](https://doi.org/10.1093/emboj/cdg113) (cit. on pp. 1, 2, 4, 11, 12).
- [See+03] M. J. Seewald, A. Kraemer, M. Farkasovsky, C. Körner, A. Wittinghofer, and I. R. Vetter. "Biochemical Characterization of the Ran–RanBP1–RanGAP System: Are RanBP Proteins and the Acidic Tail of RanGAP Required for the Ran–RanGAP GTPase Reaction?" In: *Molecular and Cellular Biology* 23.22 (Nov. 2003), pp. 8124–8136. DOI: [10.1128/mcb.23.22.8124-8136.2003](https://doi.org/10.1128/mcb.23.22.8124-8136.2003) (cit. on p. 4).
- [RM05] G. Riddick and I. G. Macara. "A systems analysis of importin- α - β mediated nuclear protein import". In: *Journal of Cell Biology* 168.7 (Mar. 2005), pp. 1027–1038. DOI: [10.1083/jcb.200409024](https://doi.org/10.1083/jcb.200409024) (cit. on p. 4).
- [YM06] W. Yang and S. M. Musser. "Nuclear import time and transport efficiency depend on importin β concentration". In: *Journal of Cell Biology* 174.7 (Sept. 2006), pp. 951–961. DOI: [10.1083/jcb.200605053](https://doi.org/10.1083/jcb.200605053) (cit. on p. 7).
- [ZAH13] J. Zienkiewicz, A. Armitage, and J. Hawiger. "Targeting Nuclear Import Shuttles, Importins/Karyopherins alpha by a Peptide Mimicking the NF κ B1/p50 Nuclear Localization Sequence". In: *JAHA* 2.5 (Sept. 2013). DOI: [10.1161/jaha.113.000386](https://doi.org/10.1161/jaha.113.000386) (cit. on p. 7).
- [Wüh+14] M. Wühr, R. M. Freeman, M. Presler, M. E. Horb, L. Peshkin, S. P. Gygi, and M. W. Kirschner. "Deep Proteomics of the *Xenopus laevis* Egg using an mRNA-Derived Reference Database". In: *Current Biology* 24.13 (July 2014), pp. 1467–1475. DOI: [10.1016/j.cub.2014.05.044](https://doi.org/10.1016/j.cub.2014.05.044) (cit. on p. 7).
- [Kir+15] K. Kirli, S. Karaca, H. J. Dehne, M. Samwer, K. T. Pan, C. Lenz, H. Urlaub, and D. Görlich. "A deep proteomics perspective on CRM1-mediated nuclear export and nucleocytoplasmic partitioning". In: *eLife* 4 (Dec. 2015). DOI: [10.7554/elife.11466](https://doi.org/10.7554/elife.11466) (cit. on p. 7).
- [NPW19] T. Nguyen, N. Pappireddi, and M. Wühr. "Proteomics of nucleocytoplasmic partitioning". In: *Current Opinion in Chemical Biology* 48 (Feb. 2019), pp. 55–63. DOI: [10.1016/j.cbpa.2018.10.027](https://doi.org/10.1016/j.cbpa.2018.10.027) (cit. on p. 7).
- [Hof20] J.-H. S. Hofmeyr. "Kinetic modelling of compartmentalised reaction networks". In: 197 (Nov. 2020), p. 104203. DOI: [10.1016/j.biosystems.2020.104203](https://doi.org/10.1016/j.biosystems.2020.104203) (cit. on p. 4).
- [KKL21] J. Kalita, L. E. Kapinos, and R. Y. H. Lim. "On the asymmetric partitioning of nucleocytoplasmic transport – recent insights and open questions". In: *Journal of Cell Science* 134.7 (Apr. 2021). DOI: [10.1242/jcs.240382](https://doi.org/10.1242/jcs.240382) (cit. on pp. 4, 7, 13).

List of codes

	page	https://github.com/numpde/nct1/tree/ ...
#1	p.2	main/code/20210225-GSR/v1
#2	p.3	main/code/20210407-Rearrangement
#3	p.3	main/code/20210225-GSR/v2
#4	p.4	main/code/20210403-StickyPore/c_rangap-sequence
#5	p.5	main/code/20211018-Appli

,

3 Appendix

3.1 Minimal Ran gradient system

Here we recapitulate the minimal Ran gradient system from [GSR03, Fig. 2], cf. §2.1. The following account for the cytoplasmic species. Here, [...] abbreviates the (cytoplasmic) concentration of the complex $\text{RanBP1} \cdot \text{Ran} \cdot \text{GTP}$. Ex is an additional potentially useful flux of nuclear $\text{Ran} \cdot \text{GTP}$ to cytoplasmic $\text{Ran} \cdot \text{GDP}$, set by default to zero.

$$\frac{d}{dt}[\text{Ran} \cdot \text{GDP}]_{\text{cyt}} = F_{\text{Ran} \cdot \text{GDP}} \frac{V_{\text{nuc}}}{V_{\text{cyt}}} + \text{GAP} + \text{GAP}_{\text{RanBP1}} + \text{Ex} \frac{V_{\text{nuc}}}{V_{\text{cyt}}} \quad (13a)$$

$$\frac{d}{dt}[\text{Ran} \cdot \text{GTP}]_{\text{cyt}} = F_{\text{Ran} \cdot \text{GTP}} \frac{V_{\text{nuc}}}{V_{\text{cyt}}} - \text{GAP} - k_{\text{on}}^{\text{rbp}}[\text{RanBP1}][\text{Ran} \cdot \text{GTP}]_{\text{cyt}} + k_{\text{off}}^{\text{rbp}}[\dots] \quad (13b)$$

$$\frac{d}{dt}[\text{RanBP1} \cdot \text{Ran} \cdot \text{GTP}] = -\text{GAP}_{\text{RanBP1}} + k_{\text{on}}^{\text{rbp}}[\text{RanBP1}][\text{Ran} \cdot \text{GTP}]_{\text{cyt}} - k_{\text{off}}^{\text{rbp}}[\dots] \quad (13c)$$

The following account for the nuclear species. As in [GSR03], E denotes free RCC1.

$$\frac{d}{dt}[\text{Ran} \cdot \text{GDP}]_{\text{nuc}} = -F_{\text{Ran} \cdot \text{GDP}} + r_8[\text{IntC}] - r_1[\text{E}][\text{Ran} \cdot \text{GDP}]_{\text{nuc}} \quad (14a)$$

$$\frac{d}{dt}[\text{Ran} \cdot \text{GTP}]_{\text{nuc}} = -F_{\text{Ran} \cdot \text{GTP}} + r_4[\text{IntA}] - r_5[\text{E}][\text{Ran} \cdot \text{GTP}]_{\text{nuc}} - \text{Ex} \quad (14b)$$

The nucleotide-exchange reaction $\text{Ran} \cdot \text{GDP} + \text{GTP} \rightleftharpoons \text{Ran} \cdot \text{GTP} + \text{GDP}$ is catalyzed by RCC1. It is modeled as in [Kle+95b, Fig. 6] / [GSR03, Fig. 1] with three intermediates. Note that it depends on the availability of GDP and GTP.

$$\frac{d}{dt}[\text{IntA}] = -(r_4 + r_6)[\text{IntA}] + r_5[\text{E}][\text{Ran} \cdot \text{GTP}]_{\text{nuc}} + r_3[\text{GTP}][\text{IntB}] \quad (15a)$$

$$\frac{d}{dt}[\text{IntB}] = r_6[\text{IntA}] + r_2[\text{IntC}] - (r_3[\text{GTP}] + r_7[\text{GDP}])[\text{IntB}] \quad (15b)$$

$$\frac{d}{dt}[\text{IntC}] = -(r_2 + r_8)[\text{IntC}] + r_1[\text{E}][\text{Ran} \cdot \text{GDP}]_{\text{nuc}} + r_7[\text{GDP}][\text{IntB}] \quad (15c)$$

Constraints on the total concentration:

$$\text{Free RCC1 :} \quad [\text{E}] = \text{RCC1}_{\text{total}} - ([\text{IntA}] + [\text{IntB}] + [\text{IntC}]) \quad (16a)$$

$$\text{Free RanBP1 :} \quad [\text{RanBP1}] = \text{RanBP1}_{\text{total}} - [\text{RanBP1} \cdot \text{Ran} \cdot \text{GTP}] \quad (16b)$$

Gradient-driven fluxes from the nucleus to the cytoplasm:

$$F_{\text{Ran} \cdot \text{GTP}} = D_{\text{Ran} \cdot \text{GTP}} ([\text{Ran} \cdot \text{GTP}]_{\text{nuc}} - [\text{Ran} \cdot \text{GTP}]_{\text{cyt}}) \quad (17a)$$

$$F_{\text{Ran} \cdot \text{GDP}} = D_{\text{Ran} \cdot \text{GDP}} ([\text{Ran} \cdot \text{GDP}]_{\text{nuc}} - [\text{Ran} \cdot \text{GDP}]_{\text{cyt}}) \quad (17b)$$

RanGAP hydrolyzes the γ -phosphate of $\text{Ran} \cdot \text{GTP}$. This is more efficient when $\text{Ran} \cdot \text{GTP}$ is bound to RanBP1 [Bis+95], reducing the IC50 seven-fold [GSR03, Table I, p. 1091].

$$\text{GAP} = k_{\text{GAP}}[\text{RanGAP}]/(1 + K_{\text{GAP}}/[\text{Ran} \cdot \text{GTP}]_{\text{cyt}}) \quad (18a)$$

$$\text{GAP}_{\text{RanBP1}} = k'_{\text{GAP}}[\text{RanGAP}]/(1 + K'_{\text{GAP}}/[\text{RanBP1} \cdot \text{Ran} \cdot \text{GTP}]) \quad (18b)$$

To determine the dynamic capacity Ex at steady-state we introduce the additional equation:

$$\frac{d}{dt}\text{Ex} = k_{\text{Ex}}[\text{Ran} \cdot \text{GTP}]_{\text{nuc}}, \quad k_{\text{Ex}} := 10 \text{ s}^{-2}, \quad \text{initial} \quad \text{Ex} := 0 \text{ } \mu\text{M s}^{-1}. \quad (19)$$

(13a)	$V_{\text{nuc}} = 1.2 \text{ pl}, \quad V_{\text{cyt}} = 1.8 \text{ pl}$	[GSR03, Table II]
(13a)	initial condition $[\text{Ran} \cdot \text{GDP}]_{\text{cyt}} = 5 \mu\text{M}$	[GSR03, Table II]
(13b)–(13c)	$k_{\text{on}}^{\text{rbp}} = 0.3 \mu\text{M}^{-1} \text{ s}^{-1}, \quad k_{\text{off}}^{\text{rbp}} = 4 \times 10^{-4} \text{ s}^{-1}$	[GSR03, Supp. Table A]
(14a)–(15c)	$r_1 = 74 \mu\text{M}^{-1} \text{ s}^{-1}, \quad r_8 = 55 \text{ s}^{-1}$ $r_7 = 11 \mu\text{M}^{-1} \text{ s}^{-1}, \quad r_2 = 21 \text{ s}^{-1}$ $r_3 = 0.6 \mu\text{M}^{-1} \text{ s}^{-1}, \quad r_6 = 19 \text{ s}^{-1}$ $r_5 = 100 \mu\text{M}^{-1} \text{ s}^{-1}, \quad r_4 = 55 \text{ s}^{-1}$	[GSR03, Supp. Table A] [Kle+95b, Fig. 6]
(15a)–(15c)	$[\text{GTP}] = 500 \mu\text{M}, \quad [\text{GDP}] = 1.6 \mu\text{M}$	[GSR03, Table II]
(16a)	$\text{RCC1}_{\text{total}} = 0.7 \mu\text{M}$	[GSR03, Supp. Table B]
(16b)	$\text{RanBP1}_{\text{total}} = 2 \mu\text{M}$	[GSR03, Fig. 4]
(17a)	$D_{\text{Ran} \cdot \text{GTP}} = 0.03 \text{ s}^{-1}$	[GSR03, Table II]
(17b)	$D_{\text{Ran} \cdot \text{GDP}} = 0.12 \text{ s}^{-1}$	
(18a)	$k_{\text{GAP}} = 10.6 \text{ s}^{-1}, \quad K_{\text{GAP}} = 0.7 \mu\text{M}$	[GSR03, Supp. Table A]
(18b)	$k'_{\text{GAP}} = 10.8 \text{ s}^{-1}, \quad K'_{\text{GAP}} = 0.1 \mu\text{M}$	[GSR03, Table I]
(18a)–(18b)	cytoplasmic $[\text{RanGAP}] = 0.7 \mu\text{M}$	[GSR03, Table II / ST B]

Table 2: Constants for the “standard simulation condition” of §2.1 at 25 °C. Except for (13a), all species are initialized to zero at $t = 0$.

Condition	Affected parameters	Nuclear RanGTP, μM	Cytoplasmic RanGTP, nM	Dynamic capacity, $\mu\text{M/s}$
“Standard”	See Table 2	4.26 (4.3)	7.75 (7.7)	0.59 (0.60)
Omission of RanBP1	$\text{RanBP1}_{\text{total}} := 0$	4.27 (4.3)	8.13 (8.1)	0.59 (0.60)
200% RCC1	$\text{RCC1}_{\text{total}}$	3.95 (4.0)	7.17 (7.1)	0.59 (0.60)
50% RCC1	$\text{RCC1}_{\text{total}}$	4.31 (4.3)	7.82 (7.7)	0.58 (0.60)
10% RCC1	$\text{RCC1}_{\text{total}}$	3.59 (3.6)	6.50 (6.4)	0.46 (0.48)
1% RCC1	$\text{RCC1}_{\text{total}}$	1.40 (1.4)	2.52 (2.5)	0.075 (0.08)
GTP:GDP = 500:0	$[\text{GDP}] := 0 \mu\text{M}$	4.80 (4.8)	8.72 (8.6)	0.59 (0.60)
GTP:GDP = 500:50	$[\text{GDP}] := \frac{1}{10}[\text{GTP}]$	0.98 (0.8)	1.76 (1.5)	0.57 (0.58)
GTP:GDP = 500:500	$[\text{GDP}] := [\text{GTP}]$	0.12 (0.12)	0.22 (0.21)	0.34 (0.34)
Saturating NTF2	$D_{\text{Ran} \cdot \text{GDP}} := 0.48 \text{ s}^{-1}$	5.12 (5.1)	9.32 (9.2)	2.18 (2.2)
No NTF2	$D_{\text{Ran} \cdot \text{GDP}} := D_{\text{Ran} \cdot \text{GTP}}$	2.55 (2.5)	4.60 (4.5)	0.15 (0.16)
200% RanGAP	$[\text{RanGAP}]$	4.27 (4.3)	3.95 (3.9)	0.59 (0.60)
50% RanGAP	$[\text{RanGAP}]$	4.26 (4.3)	14.9 (14)	0.59 (0.60)
50% permeability	$D_{\text{Ran} \cdot \text{GTP}}$	4.91 (4.9)	4.44 (4.4)	0.59 (–)
200% permeability	$D_{\text{Ran} \cdot \text{GTP}}$	3.41 (3.4)	12.4 (12.3)	0.59 (–)
400% permeability	$D_{\text{Ran} \cdot \text{GTP}}$	2.46 (2.5)	18.0 (17.8)	0.59 (–)

Table 3: Steady-state concentrations for the simulation scenarios from [GSR03, Table II/III], with their results shown in brackets. Value for $D_{\text{Ran} \cdot \text{GDP}}$ is from [GSR03, Fig. 3].

4 TODO

TODOs:

1. p.1. intro
2. p.4. cf [KKL21] citing [Kle+95a] or [Kle+95b]
3. p.5. on CAS
4. p.7. refs for those numbers
5. p.7. automate insertion of this volume
6. p.7. complete section
7. p.7. Why
8. p.7. Why